



OPEN

Synthesis and preliminary biological evaluation of quinoline-chrysin hybrids against head and neck squamous cell carcinoma

Monika Kadela-Tomanek^{1✉}, Arkadiusz Sokal^{1,2}, Kamil Krzykawski^{2,3}, Marcel Madej³ & Robert Kubina^{3,4}

Chrysin belongs to natural flavonoids characterized wide spectrum of biological activity. Its use in treatment is limited by low bioavailability and rapid metabolism. The structure–activity relationship shows that introduction of substituent at C7 position of flavone scaffold increase the activity and bioavailability. In this study, a series of quinoline-chrysin hybrids was obtained. The structure of compounds was determined using spectroscopic methods. The anticancer activity of compounds was tested against neck and head squamous cell carcinoma lines (HNSCC), while the antioxidant activity was determined using DPPH method. The biological effect depends on the type of quinoline moiety. For the most active compounds, IC_{50} values as low as ~ 13.8 μM for anticancer activity and ~ 24.5 μM for antioxidant activity were observed. For the most active compounds, their effect on the expression levels of *TP53*, *BAX*, and *BCL2* genes was examined.

Keywords Chrysin, Quinoline, Head and neck cancer, Antioxidant activity, DPPH, NMR

Cancer is one of the most common causes of death around the world. According to Global Cancer Statistics, nearly 10 million people died from cancer worldwide in 2020¹. The head and neck cancers (HNC), which includes cancer localised in the oral cavity, pharynx, larynx, nasal cavity, and salivary glands, are a significant health problem, especially in low-development countries. Risk factors include tobacco use, excessive alcohol consumption, poor oral hygiene, and infection with high-risk strains of human papillomavirus (HPV)². In 2020, it is estimated that nearly 1 million new cases and almost half a million deaths were diagnosed HNC worldwide^{1,3}. Moreover, this type of cancer is characterised by low five-year survival rate as a result of late diagnosis due to nonspecific symptoms. Treatment of HNC cancer includes mainly surgery, radiation therapy, chemotherapy or a combination of chemo- and radiation therapy. Chemotherapy is used as supplementary therapy after surgery or as the only method if the localisation of cancer excludes the surgery⁴.

Substances derived from plants, both microbial and fungal are rich with sources that may lead to new compounds exhibiting high biological activity^{5,6}. According to the World Health Organization model list of essential medicines, over 60% of currently used anticancer drugs are isolated from natural sources or mimic natural products^{7–9}. The history of using natural substances started in antiquity. Traditional medicine used herbs which were characterised by “heat-clearing,” “toxin-resolving,” “blood-invigorating,” properties. The following decades showed that extracts obtained from these herbs contain flavonoids, which exhibit the antioxidant, anti-inflammatory or vasodilation effect. Flavonoids are secondary metabolite found in fruits, vegetables, tea, and plants. Structurally, they belong to the polyphenolic compound consisting of two aromatic rings (A and B) and pyran-4-one moiety (C) (Fig. 1A). Flavonoids are divided into 12 groups depending on the amount and position of hydroxyl groups at the A or/and B ring and oxidation of the C ring^{10,11}.

Flavonoids characterise a wide spectrum of biological effects. For example, flavonoids protect plants from DNA mutation and oxidation stress caused by UV light and defence against pathogens and herbivores^{12,13}. Additionally, they show high antioxidant, anti-inflammatory, anticancer, antiviral and antimicrobial activity^{14–16}.

¹Department of Organic Chemistry, Faculty of Pharmaceutical Sciences in Sosnowiec, Medical University of Silesia in Katowice, 4 Jagiellońska Str, 41-200 Sosnowiec, Poland. ²Doctoral School, Medical University of Silesia in Katowice, 15 Poniatowskiego Str, 40-055 Katowice, Poland. ³Silesia LabMed, Centre for Research and Implementation, Medical University of Silesia, in Katowice, 18 Medyków Str, 40-752 Katowice, Poland. ⁴Department of Pathology, Faculty of Pharmaceutical Sciences in Sosnowiec, Medical University of Silesia in Katowice, Ostrogórska 30, 41-200 Sosnowiec, Poland. ✉email: mkadela@sum.edu.pl

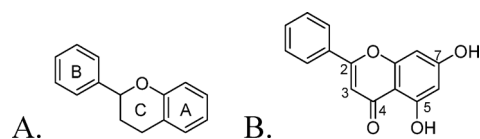


Fig. 1. The chemical structure of (A). flavonoids and (B). chrysin 1.

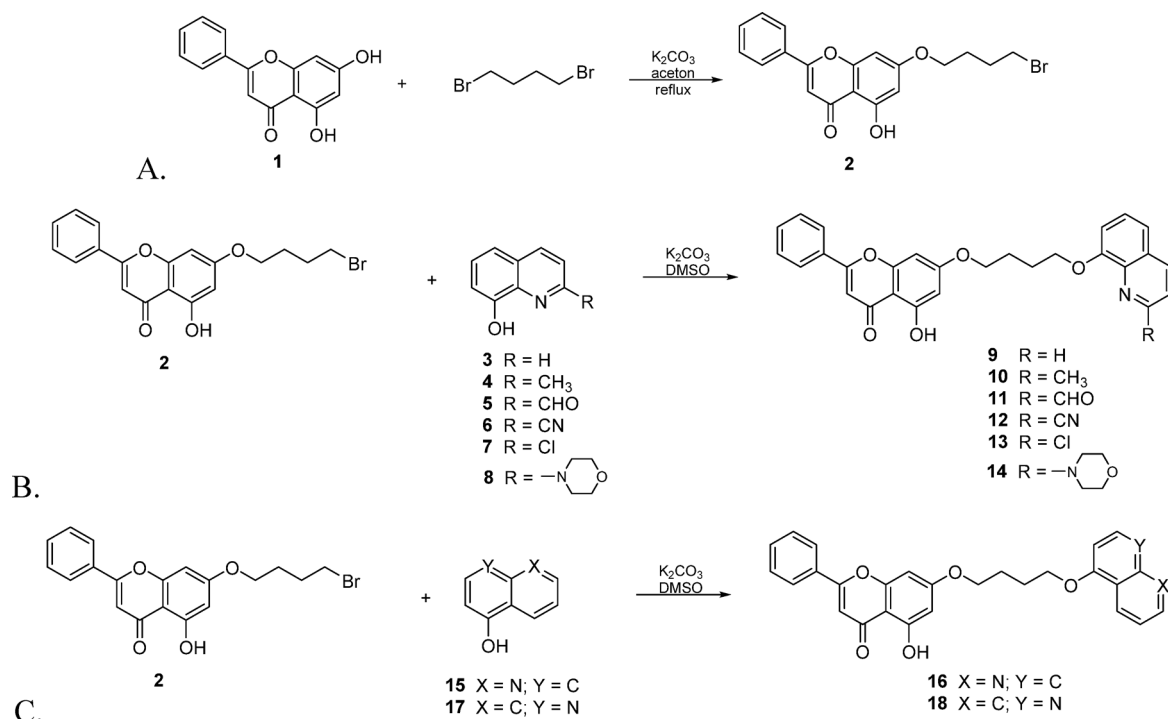


Fig. 2. The chemical synthesis of (A). 7-(4-bromobutoxy)-5-hydroxy-2-phenyl-4H-chromone-4-one **2**, (B). derivatives **9–14**, (C). compounds **16** and **18**.

Belonging to the naturally occurring flavonoid chrysin **1** is found in passion flowers (*Passiflora caerulea*), propolis and honey. The concentration of compound **1** in honey and propolis is in the range from 0.2 mg/kg to 5.3 mg/kg and from 5 g/L to 28 g/L, respectively^{17,18}. Structurally, chrysin **1** contains carbonyl group at the C4 position, a double bond between C2 and C3 carbons and two hydroxyl groups at C5 and C7 position of the flavonoid scaffold (Fig. 1B). Flavonoid **1** exhibits potent biological activity, including antioxidant, anticancer, antiviral, antidiabetic, anti-inflammatory, neuroprotective, hepatoprotective and antihyperlipidemic^{19,20}. The pharmacokinetic study shows that chrysin **1** is characterised by low oral availability which is less than 1% and is excreted in faeces. Moreover, the chrysin is rapidly metabolised to chrysin-sulphate. This is probably the reason that compound **1** shows high in vitro activity and low effect in in vivo studies²¹. Introduction of a substituent into flavone scaffold allows new compounds with high biological activity and better bioavailability than natural substance **1** to be obtained. Most of the chemical modifications are focused on replacement of one or two hydroxyl groups to ether or ester moiety. For example, introduction of methoxy group at the C5 or/and C7 position of chrysin increases lipophilicity and stability, while alkylation at the phenyl ring increases the anti-inflammatory activity and improves pharmacokinetic parameters^{22–25}.

Quinoline scaffold, which occurs in many natural and synthetic compounds, is one of the most often modified moiety in the medical chemistry. Chemically, quinoline belong to a tertiary amine base and they can reaction with electrophilic and nucleophilic compounds. Biologically, it could create hydrophobic interaction and hydrogen bond with active centre of protein, influencing their biological activity^{26,27}. Our previous research showed that introduction of quinoline moiety increased activity and bioavailability in silico of obtaining compounds^{28–30}. For this reason, we decided to connect quinoline derivatives with chrysin scaffolds. The obtained compounds were tested as anticancer substances against head and neck cancer cell lines.

Results Chemistry

As can be seen in Fig. 2A, chrysin **1** was converted into compound **2** in the reaction with 1,4-dibromobutan in the presence of potassium carbonate and acetone; the yield of the reaction was 78%³¹.

Chrysin derivative **2** was connected with 8-hydroxyquinoline derivatives **3–8**, 5-hydroxyquinoline **15** and 4-hydroxyquinoline **17**. The reaction was carried out in the presence of potassium carbonate, in dimethyl sulfoxide (DMSO) at room temperature (Fig. 2A and B). After purification on column chromatography, compounds **9–14**, **16** and **18** were obtained as the only product of reaction and the yield was 58–87%.

According to the literature, in the reaction between the 8-hydroxyquinoline and halogen compounds an ether or aryl compound could form. However, the type of product depends on the reaction conditions^{28,30,32,33}. For this reason, the structure of all compounds **9–14**, **16** and **18** was confirmed by the HR-MS, ¹H NMR, ¹³C NMR. Moreover, the 2D NMR spectra was used to determine the structure of derivatives **9**, **16** and **18** (Table S1–S3 and Figure S1–S12).

The chrysin moiety contain 15 carbon atoms and nine hydrogen atoms, whose signals were assigned based on analysis of the correlation in the HSQC and HMBC spectra (Table S1, Figure S3–S4). In the HSQC spectrum, no correlation was observed between the proton signal at δ_{H} 12.82 ppm and the carbon atom, which means that this signal belongs to the hydroxyl group at the C5 position of chrysin moiety. Additionally, the correlation between the signal at δ_{H} 12.82 ppm and δ_{C} 161.6 ppm allows us to assign this carbon signal to the C9 atom. Analysis of the multiplicity shows that only proton H3 could create a singlet signal, which is observed at δ_{H} 7.06 ppm. In the HMBC spectrum, a correlation is observed between this peak (δ_{H} 7.06 ppm) and the carbon peaks at δ_{C} 182.6 ppm, 163.9 ppm, 131.1 ppm and 105.3 ppm. The peak at δ_{H} 182.6 ppm assigned to carbon at the C4 position, because in the region up to 160.0 ppm only the peak belonging to carbonyl and carbonyloxy group was observed³⁴. In the HMBC spectrum, no correlation was observed between the chrysin moiety and protons belonging to linker and quinoline moiety (Figure S4). The analysis of 1D and 2D spectra shows, that signals at δ_{H} 4.33 ppm and δ_{H} 4.26 ppm were assigned to the methyleneoxy group at C1_L and C4_L, where the signal at δ_{H} 2.04 belonging to two methylene groups in the linker. The analysis of the HSQC spectrum shows that for all unassigned signals of protons, a correlation with carbon peaks were observed, which ether derivatives **9** were obtained in the reaction. The protons belonging to the quinoline ring were assigned based on the analysis of 2D spectra (Table S1).

Comparing the 1D and 2D NMR spectra of compounds **9**, **16**, **18** shows that the type of quinoline moiety does not increase the chemical shift of hydrogens and carbons atoms of chrysin moiety, while in the range from 4.40 ppm to 1.80 ppm three, two and four peaks for compounds **9**, **16** and **18** were observed, respectively (Table S2–S3). Therefore, the type of quinoline moiety increase the chemical shift of methylene groups at the linker.

The analysis of HSQC and HMBC spectra of compounds **16** and **18** allows the signals observed at ¹H NMR and ¹³C NMR to be assigned to the hydrogens and carbons of the quinoline moiety (Table S2–S3). Replacement of 8-hydroxyquinoline by 5-hydroxyquinoline influences the chemical shift of protons in the benzene ring of the quinoline moiety. The signal of hydrogen atoms at the C6 position have been shifted towards a high value of chemical shift due to the presence of an oxygen atom, while the signal at δ_{H} 7.09 ppm was assigned to the hydrogen atom at C7 position. Analysis of the correlation in the HMBC spectrum allows the signal at δ_{H} 7.47 ppm to be assigned to the H8 proton (Table S2). The signal of protons in the quinoline moiety of derivatives **18** were shifted towards a high value of chemical shift (Table S3).

Biological activity

One of the factors leading to head and neck cancer are smoking tobacco and alcohol consumption, which causes oxidative stress. The reactive oxygen species (ROS) interact with DNA causing uncontrolled mutations in both healthy and cancer cells. Moreover, ROS may play a role in proliferation of cancer cells through multiple pathways. Reduction of oxidative stress by neutralizing ROS may cause the inhibition of tumor growth and apoptotic induction³⁵. The antioxidants properties of compounds **1**, **9–14**, **16** and **18** were determined through analysis of the reduction of the 2,2-diphenyl-1-picrylhydrazyl (DPPH) radical. As a reference, the vitamin C substance was used. The results are presented in Table 1.

The lowest antioxidant activity in the DPPH assay is presented by chrysin **1**, which at concentration 1000 μM shows a 34.8% inhibitory effect. The series of 8-hydroxyquinoline derivatives **9–14** shows that the introduction of a substituent at the C2 position influences the antioxidant effect. Comparing the IC₅₀ shows that only compound **13** with a chloride atom at this position exhibited lower activity than derivative **9** (IC₅₀ = 36.6 \pm 1.6 μM). The position of the nitrogen atom at the quinoline moiety influences antioxidant activity, and the order is as follows **16** > **9** > **18**.

The anticancer activity of hybrid compounds **9–14**, **16**, **18**, and 5-fluorouracil (5-Fu) was evaluated against head and neck squamous cell carcinoma (HNSCC) cell lines derived from the tongue (SCC25) and the pharynx (FaDu). Cell viability was assessed using the MTT reduction assay, and the IC₅₀ values for compounds **9**, **12** and **16** were determined from dose–response curves (Table 1, Fig. 3). Effect of compounds **9**, **12**, **16**, and 5-FU on cell viability in FaDu and SCC25 cell lines depends on its concentration was presented on Figure S13.

Compounds **9–14**, **16** and **18** are characterised by moderate anticancer activity against tested cell lines. The series of compounds containing the 8-hydroxyquinoline moiety **9–14** shows that the substituent at the C2 position of the quinoline moiety increases activity. Derivatives **9**, which contain hydrogen atoms at this position depict moderate activity and the IC₅₀ is equal to 35.9 μM and 68.8 μM against SCC25 and FaDu cells, respectively. Introduction of electron-donating substituents, such as the methyl group (**10**), chloride atom (**13**) and morpholine ring (**14**), decreases the activity. Compounds with electron-withdrawing substituents (**11** and **12**) were characterised with a different activity. According to the literature, the nitrile group is a stronger electron-withdrawing group than the carbonyl group, which is related to the type of bond and to the electronegativity of the atoms^{36,37}. Introduction of a strong electron-withdrawing group, like the nitrile group, increases the anticancer activity compared to unsubstituted derivatives **9**. The series of derivatives **9**, **16** and **18** shows that introduction of the 5-hydroxyquinoline moiety increases the activity against the tested cell line, while replacement by 4-hydroxyquinoline reduces it.

Compound	X	Y	Z	R	DPPH	Cell lines/IC ₅₀ [μM]	
					IC ₅₀ [μM]	SCC25	FaDu
9	CH	CH	N	H	36.6 ± 1.6	35.9 ± 3.4	68.8 ± 4.2
10	CH	CH	N	CH ₃	34.9 ± 2.1	> 100	> 100
11	CH	CH	N	CHO	36.4 ± 2.4	> 100	> 100
12	CH	CH	N	CN	24.5 ± 1.0	30.8 ± 1.2	20.5 ± 2.4
13	CH	CH	N	Cl	51.9 ± 4.0	> 100	> 100
14	CH	CH	N		27.6 ± 3.2	> 100	> 100
16	N	CH	CH	H	26.1 ± 2.6	25.7 ± 2.8	13.8 ± 2.5
18	CH	N	CH	H	336.5 ± 6.5	> 100	> 100
1	-	-	-	-	> 1000	> 100	> 100
Vitamin C	-	-	-	-	24.4 ± 1.5	-	-
5-Fu	-	-	-	-	-	> 100	> 100

Table 1. The antioxidant and anticancer activity of compounds **1**, **9–14**, **16** and **18** and reference substance.

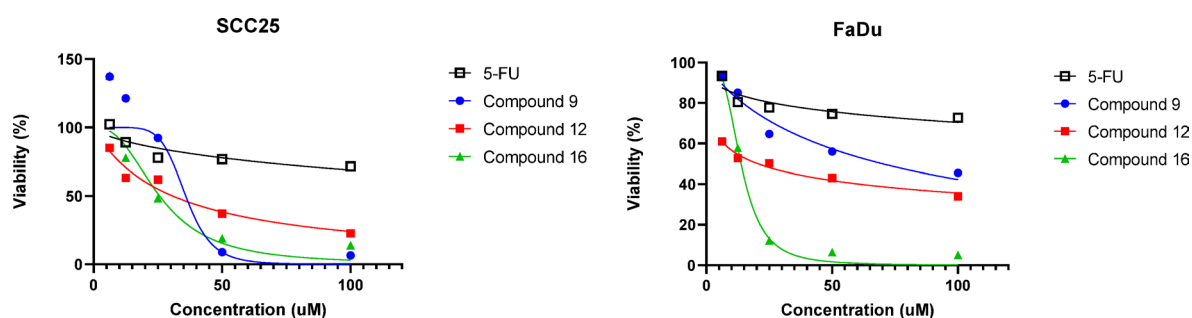


Fig. 3. Concentration-dependent effects of hybrid compounds **9**, **12**, and **16** compared with 5-FU on the viability of HNSCC cells after 48 h exposure. **(A)** SCC25 and **(B)** FaDu cell lines were treated with increasing concentrations (0–100 μM) of the indicated compounds. Cell viability was determined using the MTT assay and normalized to untreated controls. All tested derivatives reduced cell survival more effectively than 5-FU, with compound **16** showing the most pronounced cytotoxic activity in both models.

To assess whether the tested compounds modulate molecular pathways associated with apoptosis, the expression levels of the *TP53*, *BAX*, and *BCL2* genes were analysed. Compounds **12** and **16** were selected for further evaluation in both examined cell lines. The concentrations of each compound were adjusted individually based on cytotoxicity assay results. Specifically, for the FaDu cell line, concentrations of 10 μM and 15 μM were applied, while for the SCC25 line, concentrations of 20 μM and 40 μM were used. Cells were incubated with the compounds for 24 h, after which mRNA expression levels were quantified.

In FaDu cells, treatment with compound **12** at 15 μM resulted in a statistically significant upregulation of *TP53* expression compared to compound **16** at 10 μM and 15 μM ($p=0.0003$; $p=0.0006$, respectively; Fig. 4A). However, no statistically significant differences were observed when compound **12** was compared to the untreated control group ($p=0.17$), indicating that the observed effect reflects a relative difference between compounds rather than an absolute upregulation in relation to baseline expression. Notably, a slight reduction in *TP53* expression compared to control was detected following treatment with compound **16** at 10 μM, although this change did not reach statistical significance ($p=0.19$). In the SCC25 cell line, the compounds did not elicit any statistically significant changes in *TP53* expression (Fig. 4B). A decreasing trend was observed for compound **16** at 20 μM compared to control, consistent with findings in the FaDu cell line, but this effect also failed to reach statistical significance ($p=0.33$).

To further explore potential pro-apoptotic activity of the tested compounds, *BAX* gene expression was examined. In both cell lines, no significant changes in *BAX* expression were detected in any treatment group (Fig. 5A and B, respectively). Notably, even the highest concentrations of compounds **12** and **16** failed to induce any measurable upregulation or downregulation of *BAX* ($p=0.80$ for FaDu; $p=0.30$ for SCC25).

Analysis of *BCL2* expression revealed a non-significant reduction in mRNA levels in FaDu cells treated with compound **16** at 10 μM compared to untreated controls ($p=0.17$; Fig. 6A). No statistically significant alterations in *BCL2* expression were observed following treatment with compound **12** at either concentration ($p=0.61$). A

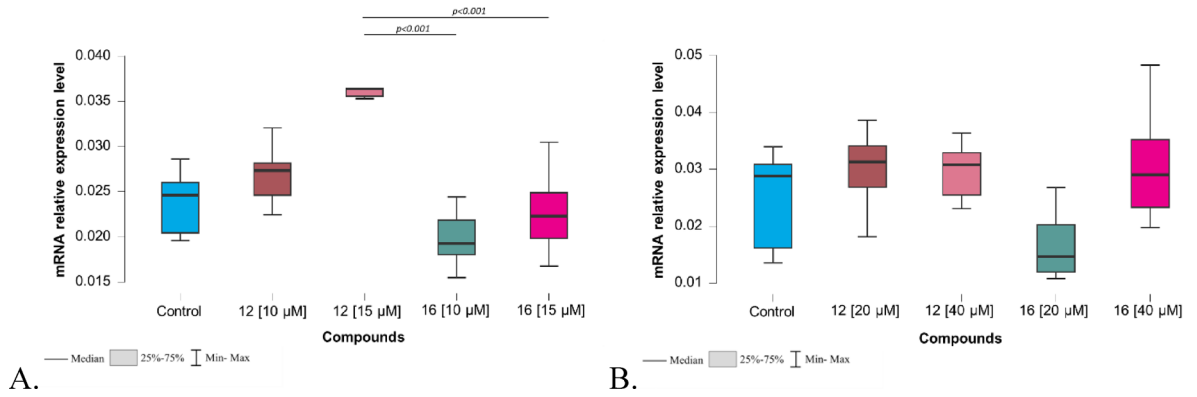


Fig. 4. Alterations in *TP53* gene expression in head and neck cancer cell lines after treatment with tested compounds. FaDu (A); SCC25 (B). Kruskal–Wallis’s test; Sample size-three biological and three technical replicates for each group; Control-untreated cells.

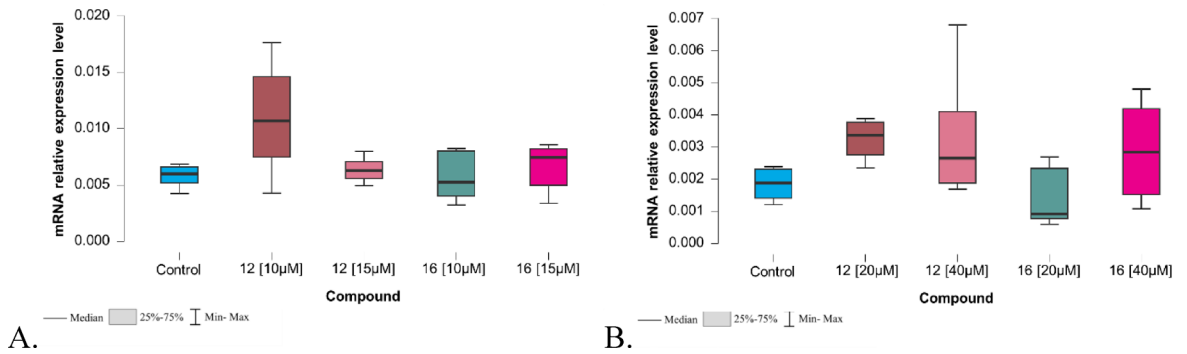


Fig. 5. Alterations in *BAX* gene expression in head and neck cancer cell lines after treatment with tested compounds. FaDu (A); SCC25 (B). Kruskal–Wallis’s test; Sample size-three biological and three technical replicates for each group; Control-untreated cells.

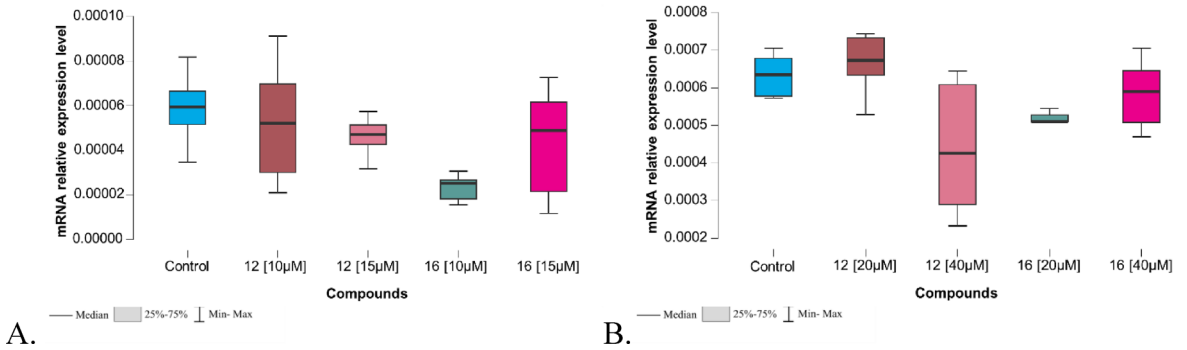


Fig. 6. Alterations in *BCL2* gene expression in head and neck cancer cell lines after treatment with tested compounds. FaDu (A); SCC25 (B). Kruskal–Wallis’s test; Sample size-three biological and three technical replicates for each group; Control-untreated cells.

comparable trend was observed in SCC25 cells, where treatment with compound 16 appeared to downregulate *BCL2* expression to a minor extent; however, these changes also did not reach statistical significance ($p = 0.28$; Fig. 6B). The expression changes observed for *TP53*, *BAX*, and *BCL2* genes were minor and did not reach statistical significance compared to untreated controls, indicating a limited transcriptional response to the tested compounds. Further mechanistic studies, including caspase activation, ROS generation, and cell cycle analyses are needed to determine whether these compounds may induce cell death via alternative pathways.

Material and methods

Chemical study

Melting points were measured using the Electrothermal IA 9300 melting point apparatus. High-resolution mass spectral analysis (HR-MS) was recorded using the Bruker Impact II instrument (Bruker, Billerica, MA, USA). The spectra were visualised using the Bruker Compass DataAnalysis 4.3 software. The theoretical value of molecular weight was determined using the online available Exact Mass Calculator³⁸. The nuclear magnetic resonance (NMR) spectra were measured using the Bruker Avance 600 spectrometer (Bruker, Billerica, MA, USA) in *d*₆-dimethyl sulfoxide solvents. Chemical shifts (δ) are reported in ppm and *J* values in Hz. Multiplicity is designated as doublet (d), doublet of doublets (dd), triplet (t) and multiplet (m). ¹H NMR and ¹³C NMR chemical shifts are reported relative to *d*₆-DMSO as an internal standard. The analysis of NMR spectra was made using MestReNova version 6.0.2 software.

All commercial substances were purchased in Merck (Darmstadt, German).

Synthesis of 7-(4-bromobutoxy)-5-hydroxy-2-phenyl-4H-chromone-4-one 2

Chrysin **1** (3.93 mmol, 1.0 g) and potassium carbonate (2.2 eqv., 8.66 mmol, 1.20 g) were dissolved in 40 mL of acetone. Next, the 1,4-dibromobutane (2.2 eqv., 8.66 mmol, 1.87 g) was added and the reaction mixture was heated to boiling temperature. After substrate disappearance on the thin layer chromatography (TLC) plate, the mixture was filtered under reduced pressure and the obtained solution was concentrated on rotary evaporator. After purification on the column chromatography (SiO₂, chloroform/ethanol, 60:1, v/v), product **2** was obtained with a yield of 78% (literature yield of 84%). The spectral data were confirmed by the literature³¹.

Synthesis of chrysin-quinoline hybrids

Compound **2** (0.257 mmol, 0.1 g) and potassium carbonate (4.4 eqv., 1.12 mmol, 0.156 g) were dissolved in 2 mL of dimethyl sulfoxide (DMSO). The solution of 8-hydroxyquinoline derivatives **3–8** (4.4 eqv., 1.12 mmol) or 5-hydroxyquinoline **15** (4.4 eqv., 1.12 mmol) or 4-hydroxyquinoline **16** (4.4 eqv., 1.12 mmol) in 2 mL of DMSO was added dropwise. After 24 h at room temperature, the reaction product was dissolved in water and extracted with methylene chloride (10 mL). The organic layer was dried with magnesium sulphate and concentrated with a vacuum evaporator. The crude product was purified by column chromatography (SiO₂, chloroform/ethanol, 15:1, v/v) to give pure products **9–14**.

5-hydroxy-2-phenyl-7-(4-(quinolin-8-yloxy)butoxy)-4H-chromone-4-one **9**: yield: 84%, mp: 193–194 °C; *R*_f: 0.64 (dichloromethane/ethanol, 15:1, v/v); ¹H NMR (600 MHz, *d*₆-DMSO) δ 2.04 (t, 4H, *J* = 3.6 Hz, 2 CH₂), 4.26 (t, 2H, *J* = 6.0 Hz, CH₂), 4.33 (t, 2H, *J* = 6.0 Hz, CH₂), 6.45 (d, 1H, *J* = 2.4 Hz, H8), 6.87 (d, 1H, *J* = 2.4 Hz, H6), 7.06 (s, 1H, H3), 7.23 (dd, 1H, *J*₁ = 1.8 Hz, *J*₂ = 7.2 Hz, H7_Q), 7.51 (d, 1H, *J* = 1.8 Hz, H5_Q), 7.52 (t, 1H, *J* = 1.8 Hz, H3_Q), 7.53 (t, 1H, *J* = 2.4 Hz, H6_Q), 7.60 (m, 2H, H3', H5'), 7.64 (m, 1H, H4'), 8.09 (m, 2H, H2', H6'), 8.30 (m, 1H, H4_Q), 8.88 (dd, 1H, *J*₁ = 1.8 Hz, *J*₂ = 4.2 Hz, H2_Q), 12.82 (s, 1H, OH) (Figure S1); ¹³C NMR (150 MHz, *d*₆-DMSO) δ 25.7 (CH₂), 26.1 (CH₂), 68.6 (2 CH₂), 93.8 (C6), 99.1 (C8), 105.3 (C10), 105.9 (C3), 109.8 (C7_Q), 120.0 (C5_Q), 122.3 (C3_Q), 126.9 (C2', C6'), 127.3 (C6_Q), 129.5 (C8A_Q), 129.7 (C3', C5'), 131.1 (C1'), 132.7 (C4'), 136.3 (C4_Q), 140.2 (C4A_Q), 149.4 (C2_Q), 154.9 (C8_Q), 157.4 (C5), 161.6 (C9), 163.9 (C2), 165.3 (C7), 182.6 (C4) (Figure S2); HRMS (*m/z*): [M + H⁺] calcd. for C₂₈H₂₄NO₅, 454.1654; found, 454.1651.

5-hydroxy-7-(4-((2-methylquinolin-8-yl)oxy)butoxy)-2-phenyl-4H-chromone-4-one **10**: yield: 79%, mp: 159–160 °C; TLC (CHCl₃:EtOH, 15:1, v/v); *R*_f: 0.66; ¹H NMR (600 MHz, *d*₆-DMSO) δ 2.07 (m, 4 H, 2 CH₂), 2.62 (s, 3 H, H2_Q'), 4.26 (t, 2H, *J* = 6.0 Hz, CH₂), 4.34 (t, 2H, *J* = 6.0 Hz, CH₂), 6.41 (d, 1H, *J* = 2.4 Hz, H8), 6.79 (d, 1H, *J* = 2.4 Hz, H6), 7.05 (s, 1H, H3), 7.18 (dd, 1H, *J*₁ = 2.4 Hz, *J*₂ = 6.6 Hz, H7_Q), 7.39 (d, 1H, *J* = 8.4 Hz, H5_Q), 7.47 (m, 2H, H3_Q, H6_Q), 7.59 (m, 2H, H3', H5'), 7.65 (m, 1H, H4'), 8.05 (m, 2H, H2', H6') 8.16 (d, 1H, *J* = 7.8 Hz, H4_Q), 12.79 (s, 1H, OH) (Figure S14); ¹³C NMR (150 MHz, *d*₆-DMSO) δ 25.5 (CH₂), 26.1 (CH₂), 68.5 (CH₂), 68.9 (CH₂), 93.7 (C6), 99.1 (C8), 105.3 (C10), 105.8 (C3), 110.0 (C7_Q), 119.8 (C5_Q), 122.8 (C3_Q), 126.2 (C8A_Q), 126.9 (C2', C6'), 127.8 (C6_Q), 129.6 (C3', C5'), 131.1 (C1'), 132.6 (C4'), 136.4 (C4_Q), 139.7 (C4A_Q), 154.4 (C8_Q), 157.6 (C2_Q), 157.8 (C5), 161.6 (C9), 163.9 (C2), 165.2 (C7), 182.5 (C4) (Figure S15); HRMS (*m/z*): [M + H⁺] calcd. for C₂₉H₂₆NO₅, 468.1811; found, 468.1807.

8-(4-((5-hydroxy-4-oxo-2-phenyl-4H-chromen-7-yl)oxy)butoxy)quinoline-2-carbaldehyde **11**: yield: 87%, mp: 183–184 °C; TLC (CHCl₃:EtOH, 15:1, v/v); *R*_f: 0.71; ¹H NMR (600 MHz, *d*₆-DMSO) δ 2.08 (m, 4 H, 2 CH₂), 4.33 (t, 2H, *J* = 6.0 Hz, CH₂), 4.37 (t, 2H, *J* = 6.0 Hz, CH₂), 6.37 (d, 1H, *J* = 2.4 Hz, H8), 6.79 (d, 1H, *J* = 2.4 Hz, H6), 7.04 (s, 1H, H3), 7.36 (dd, 1H, *J*₁ = 1.2 Hz, *J*₂ = 7.8 Hz, H7_Q), 7.59 (m, 1H, H5_Q), 7.61 (m, 2H, H3', H5'), 7.63 (m, 1H, H3_Q), 7.71 (t, 1H, *J* = 7.8 Hz, H4'), 7.93 (d, 1H, *J* = 8.4 Hz, H6_Q), 8.07 (m, 2H, H2', H6'), 8.49 (d, 1H, *J* = 8.4 Hz, H4_Q), 10.06 (d, 1H, *J* = 0.6 Hz, H2_Q'), 12.76 (s, 1H, OH) (Figure S16); ¹³C NMR (150 MHz, *d*₆-DMSO) δ 25.4 (CH₂), 25.9 (CH₂), 68.8 (CH₂), 68.8 (CH₂), 93.7 (C6), 99.0 (C8), 105.3 (C10), 105.8 (C3), 110.8 (C7_Q), 117.9 (C3_Q), 119.9 (C5_Q), 126.9 (C2', C6'), 127.8 (C6_Q), 129.6 (C3', C5', C8A_Q), 130.6 (C2_Q), 131.1 (C1'), 131.4 (C4'), 138.0 (C4_Q), 139.8 (C4A_Q), 155.5 (C8_Q), 157.7 (C5), 161.6 (C9), 163.9 (C2), 165.2 (C7), 182.5 (C4), 194.1 (CHO) (Figure S17); HRMS (*m/z*): [M + H⁺] calcd. for C₂₉H₂₄NO₆, 482.1604; found, 482.1602.

8-(4-((5-hydroxy-4-oxo-2-phenyl-4H-chromen-7-yl)oxy)butoxy)quinoline-2-carbonitrile **12**: yield: 62%, mp: 194–195 °C; TLC (CHCl₃:EtOH, 15:1, v/v); *R*_f: 0.68; ¹H NMR (600 MHz, *d*₆-DMSO) δ 2.05 (m, 4 H, 2 CH₂), 4.30 (t, 2H, *J* = 6.0 Hz, CH₂), 4.33 (t, 2H, *J* = 6.0 Hz, CH₂), 6.41 (d, 1H, *J* = 2.4 Hz, H8), 6.79 (d, 1H, *J* = 2.4 Hz, H6), 7.04 (s, 1H, H3), 7.18 (dd, 1H, *J*₁ = 0.6 Hz, *J*₂ = 7.8 Hz, H7_Q), 7.60 (m, 2H, H3', H5'), 7.67 (m, 2H, H3_Q, H5_Q), 7.73 (t, 1H, *J* = 7.8 Hz, H4'), 7.98 (d, 1H, *J* = 7.8 Hz, H6_Q), 8.08 (m, 2H, H2', H6'), 8.58 (d, 1H, *J* = 8.4 Hz, H4_Q), 12.76 (s, 1H, OH) (Figure S18); ¹³C NMR (150 MHz, *d*₆-DMSO) δ 25.5 (CH₂), 25.8 (CH₂), 68.7 (2xCH₂), 93.7 (C6), 99.0 (C8), 105.3 (C10), 105.8 (C3), 111.2 (C7_Q), 118.3 (C2_Q), 119.8 (C5_Q), 124.6 (C3_Q), 126.9 (C2', C6'), 129.6 (C3', C5'), 130.3 (C6_Q), 130.8 (C8A_Q), 131.1 (C1'), 132.6 (C4'), 138.4 (C4_Q), 140.1 (C4A_Q),

154.7 (C8_Q), 157.8 (C5), 161.6 (C9), 163.9 (C2), 165.1 (C7), 182.5 (C4) (Figure S19); HRMS (m/z): [M + H⁺] calcd. for C₂₉H₂₃N₂O₅, 479.1607; found, 479.1599.

7-(4-((2-chloroquinolin-8-yl)oxy)butoxy)-5-hydroxy-2-phenyl-4H-chromone-4-one **13**: yield: 72%, mp: 175–177 °C; TLC (CHCl₃:EtOH, 15:1, v/v): R_f = 0.74; ¹H NMR (600 MHz, d6-DMSO) δ 2.03 (m, 4 H, 2 CH_{2L}), 4.28 (t, 2H, J = 6.0 Hz, CH_{2L}), 4.31 (t, 2H, J = 6.0 Hz, CH_{2L}), 6.37 (d, 1 H, J = 2.4 Hz, H8), 6.83 (d, 1 H, J = 2.4 Hz, H6), 7.05 (s, 1 H, H3), 7.18 (dd, 1 H, J₁ = 1.2 Hz, J₂ = 7.2 Hz, H7_Q), 7.56 (m, 3 H, H3', H5', H6_Q), 7.60 (m, 2 H, H3_Q, H5_Q), 7.64 (t, 1 H, J = 7.8 Hz, H4'), 8.08 (m, 2 H, H2', H6'), 8.37 (d, 1 H, J = 8.4 Hz, H4_Q), 12.78 (s, 1 H, OH) (Figure S20); ¹³C NMR (150 MHz, d6-DMSO) δ 25.5 (CH_{2L}), 25.9 (CH_{2L}), 68.6 (CH_{2L}), 68.8 (CH_{2L}), 93.7 (C6), 99.1 (C8), 105.3 (C10), 105.8 (C3), 111.3 (C7_Q), 119.8 (C5_Q), 123.2 (C3_Q), 126.9 (C2', C6'), 128.1 (C6_Q), 128.4 (C8A_Q), 129.6 (C3', C5'), 131.1 (C1'), 132.6 (C4'), 139.4 (C4_Q), 140.3 (C4A_Q), 149.0 (C2_Q), 153.9 (C8_Q), 157.8 (C5), 161.6 (C9), 163.9 (C2), 165.2 (C7), 182.5 (C4) (Figure S21); HRMS (m/z): [M + H⁺] calcd. for C₂₈H₂₃ClNO₅, 488.1265; found, 488.1261.

5-hydroxy-7-(4-((2-morpholinoquinolin-8-yl)oxy)butoxy)-2-phenyl-4H-chromone-4-one **14**: yield: 58%, mp: 151–152 °C; TLC (CHCl₃:EtOH, 15:1, v/v): R_f = 0.67; ¹H NMR (600 MHz, d6-DMSO) δ 2.04 (m, 4 H, 2 CH_{2L}), 3.60 (m, 4 H, 2 CH_{2M}), 3.67 (m, 4 H, 2 CH_{2M}), 4.21 (t, 2H, J = 6.0 Hz, CH_{2L}), 4.30 (t, 2H, J = 6.0 Hz, CH_{2L}), 6.37 (d, 1 H, J = 2.4 Hz, H8), 6.78 (d, 1 H, J = 2.4 Hz, H6), 7.05 (s, 1 H, H3), 7.09 (dd, 1 H, J₁ = 1.2 Hz, J₂ = 7.8 Hz, H7_Q), 7.16 (t, 1 H, J = 7.8 Hz, H5_Q), 7.18 (d, 1 H, J = 9.0 Hz, H4_Q), 7.28 (dd, 1 H, J₁ = 0.6 Hz, J₂ = 8.4 Hz, H3_Q), 7.59 (m, 2 H, H3', H5'), 7.64 (m, 1 H, H4'), 8.01 (d, 1 H, J = 9.0 Hz, H6_Q), 8.06 (m, 2 H, H2', H6'), 12.79 (s, 1 H, OH) (Figure S22); ¹³C NMR (150 MHz, d6-DMSO) δ 25.7 (CH_{2L}), 25.9 (CH_{2L}), 45.5 (2 C_M), 66.5 (2 C_M), 68.6 (CH_{2L}), 68.8 (CH_{2L}), 93.6 (C6), 99.0 (C8), 105.3 (C10), 105.8 (C3), 110.3 (C7_Q), 111.6 (C6_Q), 120.0 (C5_Q), 122.6 (C3_Q), 124.4 (C8A_Q), 126.9 (C2', C6'), 129.6 (C3', C5'), 131.1 (C1'), 132.6 (C4'), 137.9 (C4_Q), 139.4 (C4A_Q), 153.1 (C8_Q), 156.8 (C2_Q), 157.8 (C5), 161.6 (C9), 163.9 (C2), 165.2 (C7), 182.5 (C4) (Figure S23); HRMS (m/z): [M + H⁺] calcd. for C₃₂H₃₁N₂O₆, 539.2182; found, 539.2172.

5-hydroxy-2-phenyl-7-(4-(quinolin-5-yloxy)butoxy)-4H-chromone-4-one **16**: yield: 86%, mp: 163–164 °C; TLC (CHCl₃:EtOH, 15:1, v/v): R_f = 0.55; ¹H NMR (600 MHz, d6-DMSO) δ 2.04 (t, 4H, J = 2.4 Hz, 2 CH_{2L}), 4.27 (m, 4H, 2 CH_{2L}), 6.42 (d, 1H, J = 2.4 Hz, H8), 6.82 (d, 1H, J = 2.4 Hz, H6), 7.06 (s, 1H, H3), 7.09 (d, 1H, J = 7.2 Hz, H7_Q), 7.42 (m, 1H, H8_Q), 7.58 (d, 1H, J = 9.0 Hz, H3_Q), 7.60 (m, 2H, H3', H5'), 7.64 (m, 1H, H4'), 7.67 (t, 1H, J = 7.8 Hz, H6_Q), 8.10 (m, 2H, H2', H6'), 8.52 (d, 1H, J = 7.8 Hz, H4_Q), 8.87 (dd, 1H, J₁ = 1.4 Hz, J₂ = 4.2 Hz, H2_Q), 12.81 (s, 1H, OH) (Figure S5); ¹³C NMR (150 MHz, d6-DMSO) δ 25.7 (2 CH_{2L}), 68.7 (2 CH_{2L}), 93.8 (C6), 99.0 (C8), 105.3 (C10), 105.8 (C3), 106.1 (C7_Q), 120.5 (C4A_Q), 121.1 (C8_Q), 121.3 (C3_Q), 126.9 (C12, C6'), 129.7 (C3', C5'), 130.2 (C6_Q), 131.1 (C1'), 132.7 (C4'), 130.6 (C4_Q), 149.0 (C8A_Q), 151.1 (C2_Q), 154.4 (C5_Q), 157.8 (C5), 161.6 (C9), 163.9 (C2), 165.1 (C7), 182.6 (C4) (Figure S6); HRMS (m/z): [M + H⁺] calcd. for C₂₈H₂₄NO₅, 454.1654; found, 454.1668.

5-hydroxy-2-phenyl-7-(4-(quinolin-4-yloxy)butoxy)-4H-chromone-4-one **18**: yield: 83%, mp: 200–201 °C; TLC (CHCl₃:EtOH, 15:1, v/v): R_f = 0.32; ¹H NMR (600 MHz, d6-DMSO) δ 1.82 (m, 2H, CH_{2L}), 1.91 (m, 2H, CH_{2L}), 4.16 (t, 2H, J = 7.2 Hz, CH_{2L}), 4.34 (t, 2H, J = 9.0 Hz, CH_{2L}), 6.07 (d, 1H, J = 8.4 Hz, H5_Q), 6.41 (d, 1H, J = 2.4 Hz, H8), 6.81 (d, 1H, J = 2.4 Hz, H6), 7.06 (s, 1H, H3), 7.39 (t, 1H, J = 7.2 Hz, H7_Q), 7.60 (t, 2H, J = 7.8, H3', H5'), 7.63 (t, 1H, J = 7.2 Hz, H4'), 7.74 (m, 1H, H6_Q), 7.80 (d, 1H, J = 8.4 Hz, H3_Q), 8.04 (m, 1H, H2_Q), 8.11 (d, 2H, J = 6.6 Hz, H2', H6'), 8.19 (dd, 1H, J₁ = 1.2 Hz, J₂ = 7.8 Hz, H8_Q), 12.81 (s, 1 H, OH) (Figure S9); ¹³C NMR (150 MHz, d6-DMSO) δ 25.6 (CH_{2L}), 25.9 (CH_{2L}), 51.9 (CH_{2L}), 68.4 (CH_{2L}), 93.8 (C6), 99.0 (C8), 105.4 (C10), 105.8 (C3), 109.2 (C5_Q), 117.1 (C3_Q), 123.7 (C7_Q), 126.3 (C8_Q), 126.9 (C2', C6'), 127.3 (C4A_Q), 129.7 (C3', C5'), 131.1 (C1'), 132.5 (C6_Q), 132.7 (C4'), 140.0 (C4_Q), 145.0 (C2_Q), 157.8 (C5), 161.7 (C9), 163.7 (C2), 165.1 (C7), 176.7 (C8A_Q), 182.5 (C4) (Figure S10); HRMS (m/z): [M + H⁺] calcd. for C₂₈H₂₄NO₅, 454.1654; found, 454.1644.

Antioxidant assay

All compounds were dissolved in DMSO (1 mg/mL). Concentrations in the range of 19–1000 μM were used for the cytotoxic assay and determination of IC₅₀ values. The antioxidant assay was determined using the previously described method^{39,40}. Briefly, the methanolic solution of DPPH (100 μL, 3 mM) was added to a 96-well plate (Nunc Thermo Fisher Scientific, Waltham, MA, USA). Then, 100 μL of the compound was added to each well. After 30 min at 25 °C, the absorption wavelength of 517 nm was measured on the BioTek 800TS microplate reader (BioKom, Poland). For all compounds, the activity was carried out at least in triplicate. The values are expressed as the percentages of radical inhibition absorbance (I%) in relation to the control values, as calculated by the following equation: I% = [(A₀ - A_S/A₀) × 100].

A₀ is the absorbance of control which exclude the test compounds, and A_S is the absorbance of the tested compounds.

Anticancer assay

Materials

Sterile dimethyl sulfoxide (DMSO cat. no. D2650) and hydrocortisone (cat. no. H6909) purchased from Merck were used. Cell culture media, fetal bovine serum, antibiotics, PBS, and trypsin were purchased in Corning (Corning Life Science, Painted Post, NY, USA). The cell lines were from the ATCC collection.

Compounds treatment

The stock solutions of derivatives **9–14**, **16** and **18** (5 mg/mL) were prepared by dissolving compounds in DMSO and then stored frozen at -80 °C until use, but no longer than 14 days. Concentrations in the range of 6.25–100 μM were used for the cytotoxic assay and determination of IC₅₀ values.

MTT test

To evaluate the cytotoxicity of the tested compounds, the MTT assay (3-[4,5-dimethylthiazol-2-yl]-2,5-diphenyltetrazolium bromide) was performed. Human head and neck squamous cell carcinoma cell lines FaDu and SCC-25 were seeded at a density of 10,000 cells per well in 96-well plates and incubated for 24 h under standard culture conditions (37 °C, 5% CO₂) in medium supplemented with 10% foetal bovine serum (FBS). Following incubation, the medium was replaced with fresh, serum-free medium containing the tested compounds at the desired concentrations. The exclusion of FBS was intended to eliminate the proliferative effects of serum-derived growth factors, thereby facilitating assessment of the compounds' direct cytotoxicity, independent of differences in cellular proliferation rates. Cells were incubated with the compounds for 48 h. After incubation, the medium was removed and replaced with medium containing MTT at a final concentration of 0.5 mg/ml. Cells were further incubated for 4 h to allow for formazan crystal formation. Subsequently, the medium was removed, and the formazan crystals were solubilised using DMSO. The resulting solutions were transferred to new 96-well plates to minimise interference from residual cellular debris. Absorbance was measured at 570 nm with background correction at 650 nm. Absorbance values obtained for compound-treated cells were normalized to untreated control cells (set as 100% viability) and expressed as percentage of cell viability. IC₅₀ values were calculated by nonlinear regression analysis using GraphPad Prism software, applying the [Inhibitor] vs. normalized response—Variable slope model. All experiments were performed in three independent biological replicates (N = 3), each including three technical replicates per condition.

Extraction and analysis of RNA

RNA was extracted from the FaDu and SCC25 cells following treatment, using the TRIzol reagent (Sigma-Aldrich, St. Louis, MO, USA) according to the protocol provided by the manufacturer. The integrity and quantity of the isolated RNA were evaluated by performing agarose gel electrophoresis and measuring absorbance with a NanoDrop OneC spectrophotometer (Thermo Scientific, Madison, WI, USA). These RNA samples were then utilised for downstream analysis of mRNA expression levels.

Evaluation of gene expression via RT-qPCR in real time

Gene expression analysis of *TP53*, *BAX*, and *BCL2* was performed using real-time reverse transcription quantitative PCR (RT-qPCR) on the QuantStudio 7 Pro Dx platform (Thermo Scientific, MA, USA). Reactions were carried out with the GoTaq[®] 1-Step RT-qPCR System (Promega, Madison, WI, USA), following the manufacturer's protocol. The *ACTB* gene (β -actin) served as the endogenous control. Relative mRNA expression levels were determined using the 2^{- $\Delta\Delta$ Ct} comparative method. Each experimental condition was assessed in three biological and three technical replicates. To ensure amplification specificity, melt curve analysis was performed, followed by verification on a 2% agarose gel. The primer sequences used for target genes are provided in Table S4.

Statistical analysis and data interpretation

Data analysis was performed by using STATISTICA software (v13.3; Tibco Inc., Palo Alto, CA, USA). All experiments were repeated three times to ensure reproducibility. Qualitative results were presented as box-and-whisker plots, created using the JASP software (version 0.19.1.0; University of Amsterdam, Amsterdam, The Netherlands). For variables not following a normal distribution, results were reported as medians accompanied by interquartile ranges. Normality of data was assessed using the Shapiro–Wilk test. Group comparisons were conducted using the Kruskal–Wallis test, a non-parametric alternative to ANOVA, followed by post hoc analysis based on mean rank differences. Statistical significance was defined as a *p*-value below 0.05.

Conclusion

In this study, we obtained new group of chrysin derivatives, which contain different quinoline moiety. New compounds are characterized by moderate antioxidant and anticancer activity. The analyses of structure–activity relationship shows that activity depend on the substituent at C2 position of quinoline moiety. Introduction of a strong electron-withdrawing group increases the activity. Moreover, the biological effect depends on the position of nitrogen atom at quinoline moiety. Effect of the compounds **12** and **16** on the expression levels of *TP53*, *BAX*, and *BCL2* genes was examined. Tested derivatives in the highest concentrations failed to induce any measurable upregulation or downregulation of *BAX*.

Data availability

The datasets used and/or analysed during the current study are available from the corresponding author on reasonable request.

Received: 20 August 2025; Accepted: 16 October 2025

Published online: 20 November 2025

References

1. Sung, H. et al. Global cancer statistics 2020: GLOBOCAN estimates of incidence and mortality worldwide for 36 cancers in 185 countries. *CA Cancer J. Clin.* **71**, 209–249 (2021).
2. Chaturvedi, A. K. et al. Human papillomavirus and rising oropharyngeal cancer incidence in the United States. *J. Clin. Oncol.* **29**, 4294–4301 (2011).
3. Marur, S. & Forastiere, A. A. Head and neck squamous cell carcinoma: Update on epidemiology, diagnosis, and treatment. *Mayo Clin. Proc.* **91**, 386–396 (2016).
4. Burney, I. Cancer chemotherapy and biotherapy: Principles and practice. *Sultan Qaboos Univ. Med. J.* **11**(3), 424–425 (2011).

5. Newman, D. J. & Cragg, G. M. Natural products as sources of new drugs over the nearly four decades from 01/1981 to 09/2019. *J. Nat. Prod.* **83**, 770–803 (2020).
6. Mazumder, A., Cerella, C. & Diederich, M. Natural scaffolds in anticancer therapy and precision medicine. *Biotechnol. Adv.* **36**, 1563–1585 (2018).
7. World Health Organization Model List of Essential Medicines–23rd List, 2023. In: *The selection and use of essential medicines 2023: Executive summary of the report of the 24th WHO Expert Committee on the Selection and Use of Essential Medicines*, 24–28. Preprint at <https://www.who.int/publications/i/item/WHO-MHP-HPS-EML-2023.02>.
8. Li, R. Natural product-based drug discovery. *Med. Res. Rev.* **36**, 3 (2016).
9. Rodrigues, T., Reker, D., Schneider, P. & Schneider, G. Counting on natural products for drug design. *Nat. Chem.* **8**, 531–541 (2016).
10. Wan, Q. et al. Therapeutic potential of flavonoids from traditional Chinese medicine in pancreatic cancer treatment. *Front. Nutr.* **11**, 1477140 (2024).
11. Dias, M. C., Pinto, D. C. G. A. & Silva, A. M. S. Plant flavonoids: Chemical characteristics and biological activity. *Molecules* **26**, 5377 (2021).
12. Treutter, D. Significance of flavonoids in plant resistance and enhancement of their biosynthesis. *Plant Biol.* **7**, 581–591 (2005).
13. Grotewold, E. The genetics and biochemistry of floral pigments. *Annu. Rev. Plant Biol.* **57**, 761–780 (2006).
14. Pietta, P. G. Flavonoids as antioxidants. *J. Nat. Prod.* **63**, 1035–1042 (2000).
15. Panche, A. N., Diwan, A. D. & Chandra, S. R. Flavonoids: An overview. *J. Nutr. Sci.* **5**, 47 (2016).
16. Kubiak, J., Szyk, P., Czarczynska-Goslinska, B. & Goslinski, T. Flavonoids, chalcones, and their fluorinated derivatives—recent advances in synthesis and potential medical applications. *Molecules* **30**, 2395 (2025).
17. Tomás-Barberán, F. A., Martos, I., Ferreres, F., Radovic, B. S. & Anklam, E. HPLC flavonoid profiles as markers for the botanical origin of European unifloral honeys. *J. Sci. Food Agric.* **81**, 485–496 (2001).
18. Bankova, V. S., de Castro, S. L. & Marcucci, M. C. Propolis: Recent advances in chemistry and plant origin. *Apidologie* **31**, 3–15 (2000).
19. Mani, R. & Natesan, V. Chrysin: Sources, beneficial pharmacological activities, and molecular mechanism of action. *Phytochemistry* **145**, 187–196 (2018).
20. Naz, S. et al. Chrysin: Pharmacological and therapeutic properties. *Life Sci.* **235**, 116797 (2019).
21. Gao, S. et al. Developing nutritional component chrysin as a therapeutic agent: Bioavailability and pharmacokinetics consideration, and ADME mechanisms. *Biomed. Pharmacother.* **142**, 112080 (2021).
22. Lee, Y. et al. Exploring the anti-inflammatory potential of novel chrysin derivatives through cyclooxygenase-2 inhibition. *ACS Omega* **9**, 50491–50503 (2024).
23. Park, M. H. et al. Anticancer effect of tectochrysin in colon cancer cell via suppression of NF-kappaB activity and enhancement of death receptor expression. *Mol. Cancer.* **14**, 124 (2015).
24. Bae, J., Kumazoe, M., Park, S. J., Fujimura, Y. & Tachibana, H. The anti-cancer effect of epigallocatechin-3-O-gallate against multiple myeloma cells is potentiated by 5,7-dimethoxyflavone. *FEBS Open Bio* **13**, 2147–2156 (2023).
25. Sokal, A. et al. Anticancer activity of ether derivatives of chrysin. *Molecules* **30**, 960 (2025).
26. Yadav, P. & Shah, K. Quinolines, a perpetual, multipurpose scaffold in medicinal chemistry. *Bioorg. Chem.* **109**, 104639 (2021).
27. Moor, L. F. E., Vasconcelos, T. R. A., Reis, R., Pinto, L. S. S. & da Costa, T. M. Quinoline: An attractive scaffold in drug design. *Mini Rev. Med. Chem.* **21**, 2209–2226 (2021).
28. Kadela-Tomanek, M., Jastrzębska, M., Chrobak, E., Bębenek, E. & Latocha, M. Hybrids of 1,4-quinone with quinoline derivatives: Synthesis, biological activity, and molecular docking with DT-diaphorase (NQO1). *Molecules* **27**, 6206 (2022).
29. Kadela-Tomanek, M., Jastrzębska, M., Chrobak, E. & Bębenek, E. Lipophilicity and ADMET analysis of quinoline-1,4-quinone hybrids. *Pharmaceutics* **15**, 34 (2022).
30. Sokal, A., Wrzalik, R., Latocha, M. & Kadela-Tomanek, M. The 8-Hydroxyquinoline derivatives of 1,4-naphthoquinone: Synthesis, computational analysis, and anticancer activity. *Int. J. Mol. Sci.* **26**, 5331 (2025).
31. Mistry, B. M., Patel, R. V., Keum, Y. S. & Kim, D. H. Chrysin-benzothiazole conjugates as antioxidant and anticancer agents. *Bioorg. Med. Chem. Lett.* **25**, 5561–5565 (2015).
32. Joaquim, A. R. et al. Identification of antimycobacterial 8-hydroxyquinoline derivatives as in vitro enzymatic inhibitors of Mycobacterium tuberculosis enoyl-acyl carrier protein reductase. *Bioorg. Chem.* **151**, 107705 (2024).
33. Li, L. et al. Discovery of novel 8-hydroxyquinoline derivatives with potent in vitro and in vivo antifungal activity. *J. Med. Chem.* **66**, 16364–16376 (2023).
34. Hermann, C., Morrill, T., Shriner, R. Fuson, R. *Systematic identification of organic compounds*, 9th ed. (Wiley, 2023).
35. You, A. J., Park, J., Shin, J. M. & Kim, T. H. Oxidative stress and dietary antioxidants in head and neck cancer. *Antioxidants* **14**, 508 (2025).
36. Lee, S. W. et al. Effect of electron-withdrawing fluorine and cyano substituents on photovoltaic properties of two-dimensional quinoxaline-based polymers. *Sci. Rep.* **11**, 24381 (2021).
37. Muhasina, P., Binoy, A. & Parameswaran, P. Correlation between bonding, philicity and substituent effects in cyclopropenylenes. *Comput. Theor. Chem.* **1205**, 113437 (2021).
38. Scientific Instrument Services (SIS) Exact mass calculator, single isotope version. Preprint at <http://www.sisweb.com/referencetools/exactmass.htm> (2025).
39. Sirivulkovit, K., Nouanthavong, S. & Sameenoi, Y. Paper-based DPPH assay for antioxidant activity analysis. *Anal. Sci.* **34**, 795–800 (2018).
40. Baliyan, S. et al. Determination of antioxidants by DPPH radical scavenging activity and quantitative phytochemical analysis of *Ficus religiosa*. *Molecules* **27**, 1326 (2022).

Author contributions

M.K.-T. designed the research work, synthesized and purified the compounds, and wrote the manuscript. A.S. synthesized and purified the compounds, and carried out analysis of spectra. K.K. and M.M performed the biological tests. R.K. supervised the biological tests. All authors reviewed the manuscript.

Funding

This research was funded by the Medical University of Silesia, grant number BNW-2-107/N/4/F and Project European Funds for Silesia 2021–2027, entitled. “Supporting the transformation of the region by strengthening the potential of the Doctoral School of the Medical University of Silesia in Katowice”: NWD/2464/2024.

Declarations

Competing interests

The authors declare no competing interests.

Additional information

Supplementary Information The online version contains supplementary material available at <https://doi.org/10.1038/s41598-025-25024-1>.

Correspondence and requests for materials should be addressed to M.K.-T.

Reprints and permissions information is available at www.nature.com/reprints.

Publisher's note Springer Nature remains neutral with regard to jurisdictional claims in published maps and institutional affiliations.

Open Access This article is licensed under a Creative Commons Attribution-NonCommercial-NoDerivatives 4.0 International License, which permits any non-commercial use, sharing, distribution and reproduction in any medium or format, as long as you give appropriate credit to the original author(s) and the source, provide a link to the Creative Commons licence, and indicate if you modified the licensed material. You do not have permission under this licence to share adapted material derived from this article or parts of it. The images or other third party material in this article are included in the article's Creative Commons licence, unless indicated otherwise in a credit line to the material. If material is not included in the article's Creative Commons licence and your intended use is not permitted by statutory regulation or exceeds the permitted use, you will need to obtain permission directly from the copyright holder. To view a copy of this licence, visit <http://creativecommons.org/licenses/by-nc-nd/4.0/>.

© The Author(s) 2025